EFFECT OF WIND TURBINE DESIGNED FOR ELECTRIC VEHICLES ON AERODYNAMICS AND ENERGY PERFORMANCE OF THE VEHICLE

by

***Emin EL*[a*], *Cengiz YILDIZ*[b], *Besir DANDIL*[c], *and Ahmet YILDIZ*[d]**

[a] Technical Sciences Vocational School, Department of Electricity and Energy, Bitlis Eren University, Bitlis, Turkey
[b] Department of Mechanical Engineering, Faculty of Engineering, Fırat University, Elazıg, Turkey
[c] Department of Mechatronics Engineering, Faculty of Engineering and Natural Sciences, Iskenderun Technical University, Hatay, Turkey
[d] Department Mechatronics Engineering, Faculty of Engineering, Fırat University, Elazıg,Turkey

Original scientific paper
https://doi.org/10.2298/TSCI2204907E

This study aims to generate, independently from the electric network, one part of the electrical energy required in the existing electric vehicles, utilizing the wind energy raised by on-the-go vehicles and thus enhancing the distance covered at one single charge. Regarding that aim, the effect of vehicle type wind turbine, which was designed so as not to cause an increase in the vehicle projection area, on the aerodynamic performance and energy efficiency of the vehicle was analyzed numerically. Using the shear stress transport k-ω turbulence model, CFD simulations were conducted to determine the drag coefficients, pressure contours and velocity vectors of the designed basic vehicle model (M0) and its two different modified versions (M1, M2). The ANSYS-FLUENT software was used for numerical simulations. In the data obtained from the simulation results, the drag coefficient, compared to the M0 model, was determined to undergo an increase by 8.49% and 4.05%, respectively for M1 and M2 models. The total energy loss of the M2 model increased by 2.47% compared to the M0 model. The net energy gain produced through the wind turbine in the M2 model constituted approximately 5.13% of the total lost energy of the M0 model vehicle. In this context, the energy gain yielded from the wind turbine placed on the vehicle was observed to be higher than the wind turbine-caused energy loss. Thus, it was determined that the study positively contributed to the prolongation of the vehicle driving distance on a single charge.

Key words: *electric vehicle, range, aerodynamic, wind energy, energy efficiency, numerical analysis*

Introduction

In parallel with the population growth and developing technology in the world, the increased living standards have increased energy consumption as well. Currently, countries meet most of their energy demand through fossil fuels. Being available in limited quantities on earth, fossil energy resources will decrease in a certain period, accordingly, their availability will go down due to the increasing price depending on that decrease, and eventually, they will be consumed up. On the other hand, high gas emissions due to fossil fuel energy use result in global warming and excessive environmental pollution [1, 2].

* Corresponding author, e-mail: eel@beu.edu.tr

One of the most common uses of fossil fuels worldwide is the land vehicles. Since about 99% of land vehicles yield the required movement energy through internal combustion engines, oil and gas are used as energy sources in these types of engines. The finiteness of these energy resources in the world urges countries to take various measures due to the damage they cause to the environment and supply security. Those measures taken by the countries push land-vehicle-producer companies away from the production of fossil fuel-consuming vehicles. Through the decisions they take, especially developed countries plan to end the production of internal combustion vehicles after a while. As a result, today, all the manufacturing companies have sped up their electric vehicle production/production planning [3-5].

In electric vehicles, propulsion is provided by electric motors. Electrical energy-storing batteries yield the needed movement energy and do not need to burn any fuel. Therefore, no emissions occur either. Albeit all these superior features, the electric vehicles have high purchasing costs and are short-range due to the issues about the storage of the energy. That poses a substantial problem. Today, the range issue continues to be a challenge for electric vehicles and limits the spread of these vehicles [6-8].

Studies on the electric vehicles' range problem focus on two primary areas. The first one is producing batteries of higher specific energy and yielding electrical energy from other sources [9-12]. The second one focuses on reducing the energy losses of the vehicle and partially recovering the lost energy. Some of the lost energy recovery methods deal with braking energies, suspension energies, and waste heat recovery systems [13-15]. Additionally, while traveling, the energy loss due to resistance forces acting in opposite direction with the vehicle and with a certain angle of attack on the vertical axis of the vehicle can be recovered, and thus, the range can be enhanced [16, 17]. Using RES is substantial for the energy supply in electric vehicles. Widespread use of solar energy systems, one of the renewable energy sources, does not seem applicable at present, especially in vehicles, due to dependence on weather, low efficiency, and requirement for large areas. Therefore, in case eco-friendly wind turbine-reinforced electricity generation systems, operating continuously and efficiently in vehicles, are used, vehicles' energy efficiency can be enhanced, and the range issue thus can be solved.

In the literature, there are very few studies on energy efficiency and range increase achieved using wind turbine systems in vehicles. It has been observed that some researches on minimizing the energy loss and recovering some of the lost energy were carried out. Lv *et al*. [18] experimentally investigated the effect of regenerative braking on the energy efficiency of an electric vehicle. Considering regenerative braking energy, they analyzed a vehicle's energy flow and compared it with another without regenerative braking. Experimental results have shown that the contribution rates of regenerative braking to energy efficiency improvement and driving range extension increased up to 11.18% and 12.58%, respectively. Long *et al*. [19] developed a new dual-actuator regenerative active suspension system for an in-wheel motor electric vehicle. The results showed that the driving comfort on different roads at 20 m/s speed was improved by approximately 52% and the dynamic performance was enhanced by 14% compared to the passive suspension. Karana and Sahoo [20] conducted the energy and exergy analysis of a thermoelectric-based waste heat recovery system of a car. The results revealed that energy efficiency could be improved up to 5.78% through the utilization of waste heat recovery. Yildiz and Dandil [21] investigated the effects of grilles on aerodynamic drag coefficient and energy loss in a vehicle. Results indicated that the grilles placed in front of the vehicle increased the aerodynamic drag coefficient by 3.71% compared to the vehicle model with no grille, and thus, the aerodynamic energy loss of the vehicle increased.

In the present study, the effect of the vehicle type wind turbine, designed to yield electrical energy from the wind energy generated in traveling vehicles, on vehicle aerodynamic performance and vehicle energy efficiency was numerically investigated. In the relevant literature, any similar study has not been come across. In the study, which is original in this respect, the effect of the designed wind turbine on the vehicle traveling 100 km at a constant speed of 27 m/s was investigated. In this context, three different vehicle models have been created. The CFD simulations were performed, using the SST *k-ω* turbulence model, to determine the drag coefficients, pressure contours, air-flow streamlines along the vehicle body, and velocity vectors of the designed models. The ANSYS-FLUENT software was used in numerical simulations, and the results were presented.

Governing equations

Resistance forces and numerical analysis

Researches in electric vehicle technologies mostly focus on the production of batteries with higher specific energy, the yield of electrical energy from other sources, the reduction of vehicle losses, and the recovery of some of the lost energy. One way to reduce the losses in vehicles is to reduce the resistance forces such as wheel rolling resistance, aerodynamic drag resistance, trailer resistance, driveline resistance, inertia resistance, and incline resistance. In the study, the aerodynamic drag resistance of the produced vehicle-type-wind turbine and the effect of this resistance on energy efficiency were investigated. The aerodynamic drag force is expressed as proportional to the square of the vehicle speed [22]:

$$F_{\mathrm{d}} = \frac{1}{2}\rho A V^2 C_{\mathrm{d}} \tag{1}$$

Accordingly, starting out from the aforementioned equation, the aerodynamic drag coefficient can be arranged [23]:

$$C_{\mathrm{d}} = \frac{F_{\mathrm{d}}}{\frac{1}{2}\rho A V^2} \tag{2}$$

The work done against the aerodynamic drag force is expressed:

$$E_1 = F_{\mathrm{d}} s = \frac{1}{2}\rho A V^2 C_{\mathrm{d}} s \tag{3}$$

The work done during the acceleration of a vehicle with a mass, M, from a rest state to velocity, V, can be written:

$$E_2 = \frac{1}{2} M V^2 \tag{4}$$

If the distance s is traveled during this time, the work done against the rolling resistance (for aerodynamic lift = 0) is formulated:

$$E_3 = P \times s = W \times f \times s \tag{5}$$

The work done against the aerodynamic drag force for the same distance is expressed as in eq. (6). Accordingly, the total energy loss is calculated:

$$E_{\mathrm{total}} = \frac{\left(E_1 + E_2 + E_3\right)}{\eta} \tag{6}$$

The power yielded out of the turbine in the car that has been mounted the turbine system on is determined by the expression [24]:

$$P_{\text{tur}} = \frac{1}{2}\rho A V^3 C_{\text{p}} \tag{7}$$

Considering the running time of the vehicle; the energy yielded out of the turbine is calculated:

$$E(J) = P(W) \times t(s) \tag{8}$$

In this study, ANSYS-FLUENT software, a widely accepted calculationol, working with the finite volume method in numerical simulations, was used. The fluid-flow was assumed to be continuous, incompressible, and turbulent. For this case, the Navier-Stokes (NS) equation was solved. Due to the incapability of the NS equation predict fluid-flows at high Reynolds numbers, a turbulence model was included in the equation system. The CFD simulations were conducted using the SST k-ω turbulence model. Then, drag coefficients, pressure contours, air-flow lines along the vehicle body, and velocity vectors of the designed car models were determined.

Model geometry and numerical method

Geometry of the cars

In the study, the effect of the designed wind turbine on the vehicle traveling 100 km distance at a constant speed of 27 m/s was investigated. In this context, three different vehicle models were created. Solidworks and SpaceClaim software were used in those models. The base vehicle model was labeled as M0. That model had an overall length of 4625 mm, a width of 1730 mm, and a height of 1482 mm. Several modifications were made to the base model M0. With each modification made, a novel model was created. The created models were named M1, M2. Figure 1 depicts isometric views of the base model and all the other modified models.

Figure 1. Basic and improved vehicle models; (a) M0, (b) M1, and (c) M2

The M0 model, to be applied flow analysis, was designed as the base model. Grilles were used in the front panel and front bumper of the model. A rectangular duct (1200 mm × 1000 mm × 530 mm) was prepared for the lower part of the model. The M1 modification was made by drilling a circular hole with a diameter of 510 mm in the front of the M0 model, fig. 2. As for the M2 modification, a previously designed wind turbine was embedded in the circular hole opened in the frontal part of the vehicle.

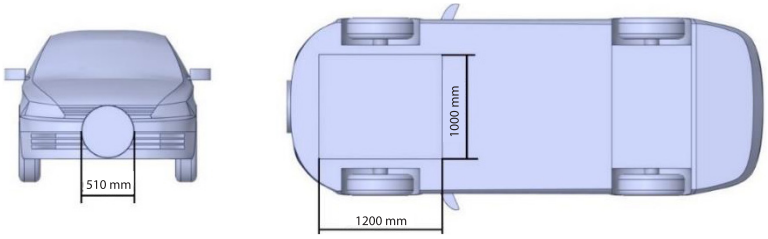

Figure 2. The model M1

Geometry of the wind turbine

The required power for the vehicle-type horizontal axis wind turbine design was assigned as 500 W. A three-bladed and 500 mm diameter wind turbine, having that power value, operating at 27 m/s wind speed (0-27 m/s wind speed range) was designed. Then, a 3-D solid model of the wind turbine was created using SOLIDWORKS software, fig. 3.

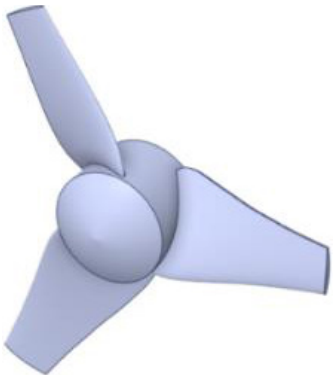

Figure 3. Vehicle type wind turbine

Grid strategy

The meshing process is important for the analyzes to give a good result. Therefore, as shown in fig. 4 in the study, smaller element sizes were used for the vehicle region where the effect of drag coefficient would be examined, while larger element sizes were used in other regions. Thus, a more accurate approach was achieved in the analysis results and the solution time of the software was shortened. The surface of the full-scale car was split into triangular elements. Additionally, a grid independence study was conducted to confirm that the element size did not affect the results. The variation of the drag coefficient was analyzed following six different mesh structures. Grid independence studies revealed that the drag force converged at approximately 672541 nodes and 3749698 elements.

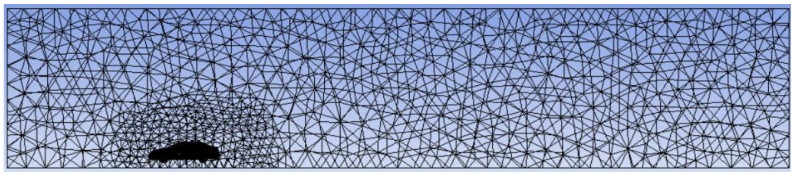

Figure 4. Triangular mesh structure of the model

Computational domain and boundary conditions

The size of the calculation area was defined as the length, L, width, W, height, H, of the vehicle. Dimensions were designated as two times the vehicle length from the front of the vehicle model, eight times at the back, two times above, and one time at each side. The length ($8L$) from the rear of the vehicle model to the exit was given to ensure a stable convergence in the drag coefficient at the end of the simulation. Figure 5 shows the side and front views of the calculation area. Reference values, boundary conditions, and solver settings are as given in tab. 1.

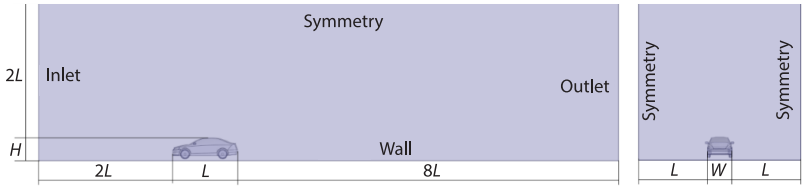

Figure 5. Domain dimensions

Table 1. Reference values, boundary condition, and solver setting

Reference values		
1	Dynamic viscosity	$1.789 \cdot 10^{-5}$ Pa·s
2	Density	1.225 kg/m^3
3	Reference area	2.98 m^2
4	Vehicle mass	1200 kg
5	Rolling resistance	0.02
Boundary conditions		
1	Velocity inlet	27 m/s
2	Bottom of domain and vehicle wall	No slip
3	Pressure outlet	Atmospheric pressure
4	Side and top outlet	Symmetry
5	Fluid	Air
6	Turbulent intensity	5%
7	Viscosity ratio	10%
Solver Settings		
1	Turbulence model	SST k-ω
2	Coupling	Pressure-velocity
3	Scheme	Simple
4	Gradient	Least squares cell based
5	Pressure	Second order
6	Momentum	Second order upwind
7	Turbulent kinetic energy	Second order upwind
8	Turbulent dissipation rate	Second order upwind

Results and analyses

In this section, using ANSYS-FLUENT software, at a speed of 27 m/s for each vehicle model of the designed modification, analyzes have been performed. During those analyzes, speed contours, static pressure contours, aerodynamic resistance coefficients affecting vehicle models have been found out, and the obtained values have been interpreted. Additionally, an analysis regarding the determination of the effect of the vehicle-type wind turbine, which will be applied to vehicles, on vehicle energy performance has been presented.

Speed contours, static pressure contours, and aerodynamic resistance coefficients affecting the model car were determined through the FLUENT program and the values obtained are given below. In fig. 6, isometric, front, and side views of the static pressure distribution and the speed vectors for the M0 vehicle model are depicted.

The pressure on the frontal vehicle surfaces, which were directly exposed to the wind while traveling, was observed to be high, fig. 6(a). The maximum pressure occurred in the front bumper area of the vehicle and was calculated as 452.2 Pa. Isometric, side and front views of the velocity vectors of the M0 model are given in fig. 6(b). The speed were seen to form to cover the vehicle surface geometry. The wind speed was detected to increase towards the upper parts of the vehicle. At the end of the solution process, the aerodynamic drag coefficient of the M0 model was found to be $C_d = 0.2814$.

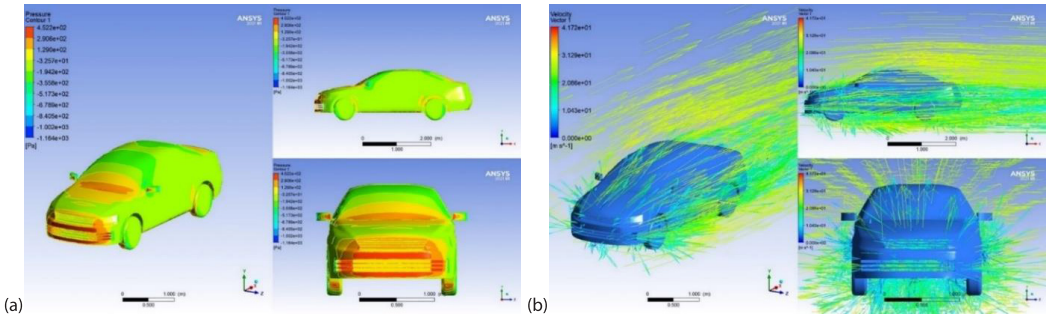

Figure 6. Isometric, side, and front views for the static pressure contour; (a) and speed vectors and (b) of the M0 model vehicle

Figure 7 depicts isometric, front, and side views for the static pressure distribution and the speed vectors of the M1 vehicle model.

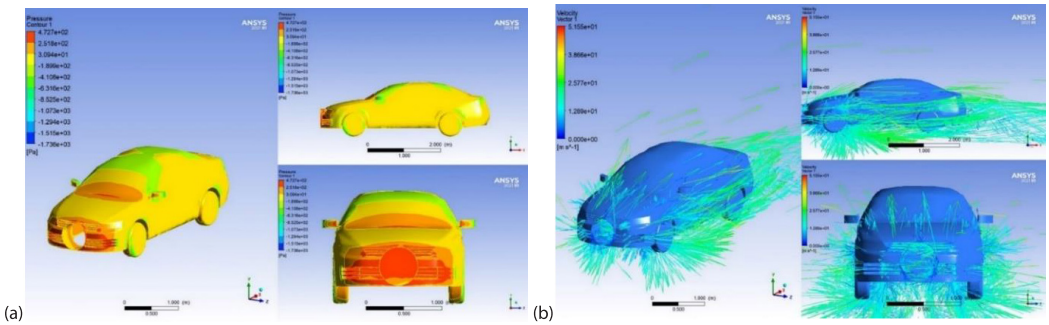

Figure 7. Isometric, side, and front views for the static pressure contour; (a) and the speed vectors (b) of the M1 model vehicle

The pressure on the M1 model vehicle's front surfaces, directly exposed to the wind while traveling, was observed to be high, as in the M0 model, fig. 7(a). The maximum pressure occurred in the front bumper area and was calculated as 472.7 Pa. Isometric, side, and front views for the velocity vectors of the M1 model are given in fig. 7(b). As a result of the solution process, the aerodynamic drag coefficient of the M1 model was found to be $C_d = 0.3053$.

The isometric, side, and front views for the static pressure distribution and the speed vectors of the M2 vehicle model are as depicted in fig. 8.

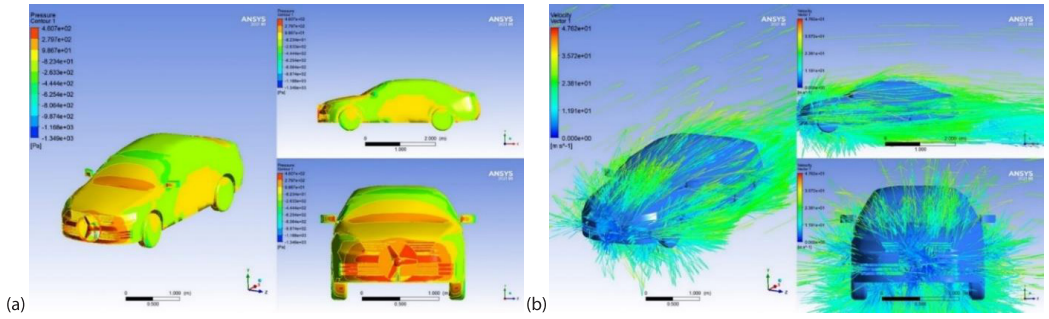

Figure 8. Isometric, side, and front views for the static pressure contour; (a) and the speed vectors (b) of the M2 model vehicle

The pressure on the M2 model vehicle's front surfaces, directly exposed to the wind while traveling, was observed to be high, as well, fig. 8(a). The maximum pressure occurred in the front bumper area and was calculated as 460.7 Pa. Isometric, side, and front views for the velocity vectors of the M2 model are given in fig. 8(b). As a result of the solution process, the aerodynamic drag coefficient of the M2 model was found to be $C_d = 0.2928$.

The drag coefficients, C_d, of the M0, M1, and M2 models were, respectively calculated as 0.2814, 0.3053, and 0.2928. Of all the models, the M0 had the lowest drag coefficient value. The drag coefficients of the M1 and M2 models increased by 8.49% and 4.05%, respectively. The M1 model was determined to have the highest drag coefficient value compared to the other models.

The energy losses that the vehicle models went through depending on their aerodynamic structures were calculated using eq. (3). As a result of the calculations, the aerodynamic energy amounts consumed in the M0, M1, and M2 models were found to be 37443.3 kJ, 40623.4 kJ, and 38960.2 kJ, respectively, fig. 9(a). Accordingly, the highest aerodynamic energy loss occurred in the M1 model.

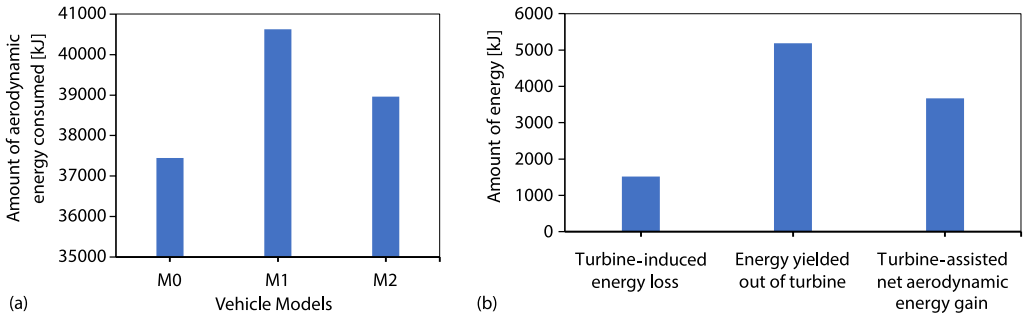

Figure 9. (a) Aerodynamic energy consumption while traveling a 100 km distance at a speed of 27 m/s and (b) aerodynamic energy loss-gain status for the wind turbine-installed-model in comparison with the base model

As seen in fig. 9(a), modifying the base model (M0), drilling a circular hole on the vehicle (M1), and embedding a wind turbine into the hole (M2) caused the amount of aerodynamic energy consumed, and thus fuel consumption increase. In terms of aerodynamic energy loss, there occurred an increase by 4.05% in the model with wind turbine (M2), about the base model (M0).

In the model with a wind turbine system (M2), the energy yielded out of the turbine was calculated using eqs. (7) and (8). The energy obtained from the turbine was determined to be higher than the turbine-related energy loss. In this context, the aerodynamic energy loss in the turbine model compared to the base model, the energy obtained from the turbine, and the gain in the amount of aerodynamic energy supplied by the turbine in the wind-turbine-installed model are shown in fig. 9(b). In addition, the energy loss percentage in the turbine model, and the percentage of gain in the amount of energy obtained through the turbine, compared to the base model, were calculated:

$$(\%\text{Loss}) = \frac{E_{1\,\text{turbine-induced loss}}}{E_{1\,\text{base model}}} \tag{9}$$

$$(\%\text{Gain}) = \frac{E_{1\,\text{turbine-assisted gain}}}{E_{1\,\text{base model}}} \tag{10}$$

Accordingly, while the energy loss ratio was found to be 4.05% and the energy gain ratio obtained through the turbine was 9.80%. For the analyzed vehicle models, the total amount

of energy consumed for each model is given in fig. 10(a), considering the work done against the aerodynamic drag force, E_1, energy consumed, E_3, respectively.

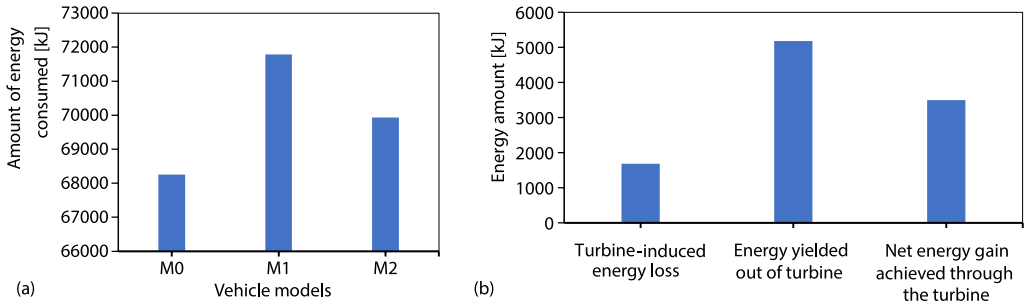

Figure 10. (a) Total amount of energy consumed while traveling a 100 km distance at a speed of 27 m/s and (b) total energy loss-gain status of the wind turbine installed model in comparison with the base model

Compared to the M0, total energy consumption, and therefore, fuel consumption increased in models M1 (with a circular hole on the front bumper) and M2 (with a turbine embedded), as depicted in fig. 10(a). In the system with a wind turbine, total energy loss increased by 4.5% in comparison with the base model. Those geometry changes made on the base model were determined to increase the aerodynamic drag coefficient and thus have an impact that increases the general fuel consumption.

In the car equipped with the turbine system, the power yielded through the turbine was found as 1400.28 W with the help of eq. (7) (for 27 m/s speed), while the amount of energy gained out of the turbine was found as 5185.24 kJ, using eq. (8). Thus, the total energy loss between the base model and the wind turbine model was determined to be 1685.44 kJ, and the energy gain of the wind turbine system was 3499.80 kJ, compared to the base model.

Within this context, compared to the base model, the energy loss in the turbine model, the energy yielded through the turbine, and the gain in the amount of energy obtained out of the turbine is shown in fig. 10(b). Additionally, for the base model, the energy loss ratio in the turbine model and the percentage of gain in the amount of energy obtained through the turbine were calculated:

$$(\%\text{Loss}) = \frac{E_{\text{turbine-induced loss}}}{E_{\text{base model}}} \tag{11}$$

$$(\%\text{Gain}) = \frac{E_{\text{turbine-assisted gain}}}{E_{\text{base model}}} \tag{12}$$

Accordingly, the amount of energy loss was found to be 2.47%, while the energy gain percentage obtained through the turbine was 5.13%.

Conclusion

In the present study, it was aimed to yield a part of the electrical energy, required in existing electric vehicles, out of the wind energy generated in on-the-go vehicles, independently of the in-vehicle electric grid, and thus to boost the distance traveled on a single charge. With that aim, the effect of the vehicle-type wind turbine, designed not to cause an increase in the vehicle projection area, on the vehicle aerodynamic performance and vehicle energy efficiency has been numerically analyzed. In the study, the effect of the designed wind turbine on the vehicle traveling

100 km distance at a constant speed of 27 m/s speed was investigated. In the analyzes and calculations performed, it has been observed that the pressure was higher on the front surfaces where the vehicle was in direct contact with the wind while traveling, and the streamlines were formed in a way to adapt to the vehicle shape. An increase in the drag resistance coefficient was observed in the M1 modification, which was designed by opening circular holes in the front bumper of the base model M0. In this case, compared to the base model, the resistance coefficient increased by 8.49% according to ANSYS Fluent data. The increase in the resistance coefficient with the hole opened in the front bumper occurred because that the pressure exerted to the front surface and thus the force applied to the vehicle in the flow direction increased. In the case of installing the wind turbine within the hole opened in the front bumper (M2), compared to the base model, the drag resistance coefficient was observed to increase by 4.05%, according to the ANSYS Fluent data. Although the increase in the resulting resistance coefficient was relatively higher than the one in the base model (M0), it was 4.09% lower than that of the model with the hole (M1). It was observed that turbine blades, which were embedded in the hole, accelerated the air-flow inward, and thus tended to dislocate the decomposition point downwards. An increase of aerodynamic energy loss occurred in the wind turbine-installed model (M2) by 4.05%, compared to the base model (M0). However, the net energy gain achieved through the wind turbine was observed to cover approximately 9.80% of the aerodynamic energy loss of the base model. The total energy loss in M1 modification increased by 5.17%, compared to the base model (M0). Likewise, in comparison with the base model, there was an increase of 2.47% in model M2. However, the net energy gain, achieved thanks to the additional wind turbine, covered approximately 5.13% of the total energy loss in the base model. Besides, it was determined that 7.41% thereabouts of the total energy loss in the turbine-installed model could be compensated with the help of the wind turbine. In this context, the energy gain thanks to the wind turbine placed on the vehicle was seen to be is higher than the wind turbine-induced energy loss. It was determined that this occurrence had the potential to contribute positively to the prolongation of the traveling distance on a single charge.

Acknowledgment

This study has been produced from the Ph. D. thesis studies of E. EL. The authors would like to thank the Scientific Research Projects Coordination Unit (FUBAP) of Firat University Rectorate for the financial support provided with project number MF.20.38.

Nomenclature

A – vehicle projection area
C_d – aerodynamic drag coefficient
C_p – turbine power coefficient
$E_{base\ model}$ – total energy loss in a base model vehicle
E_{gain} – energy gain of the wind turbine model compared to the base model
$E_{turbine\ model}$ – total energy loss in the vehicle model with wind turbine
$E_{1turbine\text{-}assisted\ gain}$ – aerodynamic energy gain of the wind turbine model compared to the base model
$E_{1turbine\text{-}induced\ loss}$ – aerodynamic energy loss between the base model and the wind turbine model
$E_{1turbine\ model}$ – aerodynamic energy loss in a model vehicle with wind turbine
$E_{turbine}$ – amount of energy gained through the turbine
$E_{turbine\ loss}$ – total energy loss between the base model and the wind turbine model
$E_{1base\ model}$ – aerodynamic energy loss in the base model vehicle
f – rolling resistance coefficient
H – height
F_d – aerodynamic drag force
L – vehicle length
M – vehicle mass
P – pressure
s – amount of distance traveled
t – time
V – velocity
W – vehicle weight

Greek symbol

ρ – density of air
η – electric vehicle efficiency

References

[1] Jacobson, M. Z., Review of Solutions to Global Warming, Air Pollution, and Energy Security, *Energy & Environmental Science*, *2* (1999), 2, pp. 148-173
[2] Ozer, S., *et al.*, Effects of Fusel Oil in a Thermal Coated Engine, *Fuel*, *306* (2021), 121716
[3] Burch, I., Gilchrist, J., *Survey of Global Activity to Phase Out Internal Combustion Engine Vehicles*, Center of Climate Protection: Santa Rosa, Cal., USA
[4] Michaelides, E. E., Primary Energy Use and Environmental Effects of Electric Vehicles, *World Electric Vehicle Journal*, *12* (2021), 3, 138
[5] Blagojević, I. A., *et al*., The Future (and The Present) of Motor Vehicle Propulsion Systems, *Thermal Science*, *23* (2019), 5, pp. 1727-1743
[6] Liu, Z., *et al.*, Comparing Total Cost of Ownership of Battery Electric Vehicles and Internal Combustion Engine Vehicles, *Energy Policy*, *158* (2021), 112564
[7] Petrović, Đ. T., *et al*.,. Electric Cars: Are They Solution Reduce CO_2 Emission, *Thermal Scienc*e, *24* (2020), 5 Part A, pp. 2879-2889
[8] Puma-Benavides, D. S., *et al*., A systematic Review of Technologies, Control Methods, and Optimization for Extended-Range Electric Vehicles, *Applied Sciences*, *11* (2021), 15, 7095
[9] Tran, M. K., *et al*., A Review of Range Extenders in Battery Electric Vehicles: Current Progress and Future Perspectives, *World Electric Vehicle Journal*, 12 (2021), 2, 54
[10] Cano, Z. P., *et al*., Batteries and Fuel Cells for Emerging Electric Vehicle Markets, *Nature Energy*, *3* (2018), 4, pp. 279-289
[11] Tolmachev, Y. V., *et al.*, Energy Cycle Based on A High Specific Energy Aqueous Flow Battery and Its Potential Use for Fully Electric Vehicles and for Direct Solar-to-Chemical Energy Conversion, *Journal of Solid State Electrochemistr*y, *19* (2015), 9, pp. 2711-2722
[12] Tie, S. F., Tan, C. W., A Review of Energy Sources and Energy Management System in Electric Vehicles, *Renewable and Sustainable Energy Reviews*, *20* (2013), Apr., pp. 82-102
[13] Puma-Benavides, D. S., *et al*., A Systematic Review of Technologies, Control Methods, and Optimization for Extended-Range Electric Vehicles, *Applied Sciences*, *11* (2021), 15, 7095
[14] Xiao, B., *et al*., A Review of Pivotal Energy Management Strategies for Extended Range Electric Vehicles, *Renewable and Sustainable Energy Reviews*, *149* (2021), 111194
[15] Thanapalan, K., *et al*., Renewable Hydrogen Hybrid Electric Vehicles and Optimal Energy Recovery Systems, *Proceedings*, 2012 UKACC International Conference on Control, Cardiff, UK, 2012, pp. 935-940
[16] Ferraris, A., *et al.*, Integrated Design and Control of Active Aerodynamic Features for High Performance Electric Vehicles, SAE Technical Paper 2020-36-0079, 2021
[17] Huluka, A. W., Kim, C. H., A Numerical Analysis on Ducted Ahmed Model as a New Approach to Improve Aerodynamic Performance of Electric Vehicle, *International Journal of Automotive Technology*, *22* (2021), 2, pp. 291-299
[18] Lv, C., *et al*., Mechanism Analysis and Evaluation Methodology of Regenerative Braking Contribution Energy Efficiency Improvement of Electrified Vehicles, *Energy Conversion and Management*, *92* (2015), Mar., pp. 469-482
[19] Long, G., *et al*., Regenerative Active Suspension System With Residual Energy for In-Wheel Motor Driven Electric Vehicle, *Applied Energy*, *260* (2020), 114180, pp. 1-18
[20] Karana, D. R., Sahoo, R. R., Experimental Study on Exergy and Sustainability Analysis of the Thermoelectric Based Exhaust Waste Heat Recovery System, *International Journal of Exergy*, *34* (2021), 1, pp. 1-15
[21] Yildiz, A., Dandil, B., Investigation of Effect of Vehicle Grilles on Aerodynamic Energy Loss and Drag Coefficient, *Journal of Energy Systems*, *2* (2018), 4, pp. 190-203
[22] Wu, J. D., Liu, J. C., Development of A Predictive System for Car Fuel Consumption Using an Artificial Neural Network, *Expert Systems With Applications*, *38* (2011), 5, pp. 4967-4971
[23] Hucho, W. H., The Aerodynamic Drag of Cars Current Understanding, Unresolved Problems, and Future Prospects, in: *Aerodynamic Drag Mechanisms of Bluff Bodies and Road Vehicles*, Springer, New York, USA, 1978, pp. 7-44
[24] Yildiz, A., Dandil, B., Power Generation Potential of Small Wind Turbine in Elazig Province, Turkey, *Proceedings*, 4th International Conference on Power Electronics and Their Applications (ICPEA), Elazig, Turkey, 2019, pp. 1-6

Paper submitted: June 30, 2021
Paper revised: November 7, 2021
Paper accepted: May 13, 2022